

Mutations in *N*-acetylglucosamine (*O*-GlcNAc) transferase in patients with X-linked intellectual disability

Anke P. Willems^{1,2,#}, Mehmet Gundogdu^{3,#}, Marlies J.E. Kempers⁴, Jacques C. Giltay⁵, Rolph Pfundt⁴, Martin Elferink⁵, Bettina F. Loza⁶, Joris Fuijkschot⁷, Andrew T. Ferencbach³, Koen L.I. van Gassen^{5*}, Daan M.F. van Aalten^{3,*} and Dirk J. Lefeber^{1,2,*}

¹Department of Neurology, Donders Institute for Brain, Cognition and Behaviour, Radboud University Medical Centre, 6500 HB Nijmegen, The Netherlands. ²Department of Laboratory Medicine, Translational Metabolic Laboratory, Radboud Institute for Molecular Life Sciences, Radboud University Medical Center, 6525 GA Nijmegen, The Netherlands. ³Centre for Gene Regulation and Expression, School of Life Sciences, University of Dundee, DD1 5EH Dundee, Scotland, United Kingdom. ⁴Department of Genetics, Radboud University Medical Center, 6500 HB Nijmegen, the Netherlands. ⁵Department of Genetics, University Medical Centre Utrecht, 3508 AB Utrecht, The Netherlands. ⁶Department of Paediatrics, VieCuri Hospital, 5900 BX Venlo, The Netherlands. ⁷Department of Paediatrics, RadboudUMC Amalia Children's Hospital, 6500 HB Nijmegen, the Netherlands

These authors contributed equally to this work:

Shared first authors

* Shared last authors

To whom correspondence should be addressed: Dirk Lefeber Dirk.Lefeber@Radboudumc.nl, Daan van Aalten dmfvanaalten@dundee.ac.uk

Keywords: glycobiology; glycosyltransferase; metabolic disease; *O*-GlcNAcylation; *O*-linked *N*-acetylglucosamine (*O*-GlcNAc) transferase (OGT); Congenital Disorders of Glycosylation; Host Cell Factor 1 (HCF-1); X-linked Intellectual Disability (XLID)

ABSTRACT

N-acetylglucosamine (*O*-GlcNAc) transferase (OGT) regulates protein *O*-GlcNAcylation, an essential and dynamic post-translational modification. The *O*-GlcNAc modification is present on numerous nuclear and cytosolic proteins and has been implicated in essential cellular functions such as signalling and gene expression. Accordingly, altered levels of protein *O*-GlcNAcylation have been associated with developmental defects and neurodegeneration. However, mutations in the *OGT* gene have not yet been functionally confirmed in humans. Here, we report on two hemizygous mutations in *OGT* in individuals with X-linked intellectual disability (XLID) and dysmorphic features: one missense mutation (p.Arg284Pro) and one mutation leading to a splicing defect (c.463-6T>G). Both mutations reside in the tetratricopeptide repeats of OGT that are essential for substrate recognition. We observed slightly reduced levels of OGT protein, and reduced levels of its opposing enzyme *O*-GlcNAcase (OGA) in both patient-derived fibroblasts, but global *O*-GlcNAc levels appeared to be unaffected. Our data suggested

that mutant cells attempt to maintain global *O*-GlcNAcylation by downregulating OGA expression. We also found that the c.463-6T>G mutation leads to aberrant mRNA splicing, but no stable truncated protein was detected in the corresponding patient-derived fibroblasts. Recombinant OGT bearing the p.Arg284Pro mutation was prone to unfolding and exhibited reduced glycosylation activity against complex array of glycosylation substrates and proteolytic processing of the transcription factor host cell factor 1 (HCF1), which is also encoded by an XLID-associated gene. We conclude that defects in *O*-GlcNAc homeostasis and HCF1 proteolysis may play roles in mediation of XLID in individuals with *OGT* mutations.

Protein *O*-GlcNAcylation is a dynamic and reversible post-translational modification that is present on many nucleocytoplasmic and mitochondrial proteins (1,2). *O*-GlcNAcylation involves cycling of a single *N*-acetylglucosamine (*O*-GlcNAc) moiety on serine and threonine residues of a spectrum of substrates, affecting their stability, activity and subcellular

localization (3,4). The transfer of *O*-GlcNAc is catalysed by *O*-GlcNAc transferase (OGT) (5,6) and is modulated by the availability of the donor substrate UDP-GlcNAc (7). UDP-GlcNAc biosynthesis is coupled to glucose, glutamine and nucleotide metabolism. Concomitantly, OGT exerts a nutrient-sensitive regulation over various cellular functions by acting on myriad targets (8). OGT is highly conserved in metazoa and consists of multiple tetratricopeptide repeats (TPRs) on the N-terminus and a C-terminal glycosyltransferase domain (9,10). While TPRs are known to be involved in protein-protein interactions, in the context of OGT they facilitate substrate recognition and specificity (11). In addition to its glycosyltransferase activity, OGT was recently shown to have a role in proteolytic processing of Host Cell Factor 1 (HCF1) (12,13), a transcriptional co-regulator of the cell cycle (14). HCF1 is heavily *O*-GlcNAcylated (15), but a recent study revealed that *O*-GlcNAcylation and proteolytic cleavage of HCF1 by OGT are independent processes (16). OGT activity is counteracted by *O*-GlcNAcase (OGA), a hexosaminidase that specifically removes *O*-GlcNAc modifications (17). It has been shown that chemical inhibition of OGA in different human cell lines leads to a decreased expression of OGT and an increased expression of OGA (18), which indicates an as yet unidentified mechanism of regulation to maintain global *O*-GlcNAc homeostasis. OGT has been linked to embryonic development in a number of animal models. *Caenorhabditis elegans* with null mutations in *ogt-1* are viable and fertile, but with metabolic defects (19). In *Drosophila*, OGT is encoded by the *super sex combs* gene, which is essential for *Drosophila* viability and segmentation (20,21). Knockdown of *OGT* in zebra fish causes impaired embryonic growth with reduced brain size (22). Although OGT is ubiquitously expressed, it is remarkably abundant in brain (9,10). Accordingly, *O*-GlcNAcylation has been linked to neuronal function and brain development in a number of cell and animal models (23),(22). In addition, recent studies have shown that *O*-GlcNAc signalling can regulate axonal and dendritic growth (24,25) and AMPA receptor trafficking (26,27), possibly affecting learning and memory processes. Also, alterations in protein *O*-GlcNAcylation have been associated with neurodegenerative diseases (28). Genetic *OGT* variants identified in patients with X-linked intellectual disability (XLID) have

previously been documented: firstly, in a clinical report, albeit accompanied by mutations in *MED12* (a known XLID gene) (29) and secondly in a large screen for novel XLID genes (30). Here, we describe two patients with intellectual disability, bearing hemizygous mutations in *OGT*. By combining characterization of the *O*-GlcNAcylation machinery in patient cells and characterisation of the effects of OGT XLID mutations on OGT dual activity *in vitro*, we provide preliminary evidence suggesting that effects on the *O*-GlcNAc proteome and proteolytic processing of HCF1 may underpin the observed XLID phenotypes.

RESULTS

Clinical phenotype of two ID patients

Two male patients showed intellectual disability and a developmental delay due to an unknown cause.

Cognitive testing in patient 1, at the age of 5 years old, showed reduced intelligence (WPPSI-III-NL, score 2;9) and delay in adaptive behaviour (VABS, score 2;0). Additional neurological symptoms were pyramidal syndrome, mild spastic diplegia and psychomotor retardation with behavioural conduct disorder. In addition, patient 1 had an inguinal hernia. Dysmorphic features included hypertelorism, low set ears, a broad nose, full lips, supernumerary nipple, hypoplastic toe, mild retrognathia, long and thin fingers, clinodactyly and microcephaly (Fig. 1A). Patient 1 showed involvement of the eyes including amblyopia and possible astigmatism. He was born with a mild respiratory insufficiency based upon transient tachypnea of the neonate. Cardiac screening revealed a bicuspid aortic valve. An MRI at the age of 2 years old showed mild abnormalities pointing towards periventricular leukomalacia (Fig. 1C), but with a normal EEG.

The global developmental level of patient 2, at the age of 5.5 years old, was estimated at 1.5 years. He showed mouth hypotonia with drooling, and involvement of the eyes including nystagmus, astigmatism and high hypermetropia. Genital abnormalities included a small phallus, and orchiopexy was performed at the age of 3 years. His dysmorphic phenotype was less evident, with bitemporal narrowing and metopic ridge as main features (Fig. 1B). Upon birth, a ventricular septal defect was detected, which closed spontaneously at later age. An MRI

performed at the age of 3 years old showed no clear brain abnormalities (Fig. 1D). Clinical features of the patients are summarized in Table 1.

Identification of mutations in OGT

Whole exome sequencing was performed in the two male patients from unrelated families to uncover the cause of their intellectual disability. Mutations in *OGT* were found in both patients.

In patient 1, trio-sequencing and filtering for *de novo* variants revealed two potential candidate genes. A heterozygous *de novo* mutation was found in bromodomain-containing protein 1 (*BRD1*): Chr22(GRCh38): g.49,823,630C>G; NM_001304808.1:c.688G>C (p.Val230Leu). In addition, a hemizygous *de novo* missense variant in *OGT* was discovered: ChrX(GRCh38): g.71,555,312G>C; NM_181672.2: c.851G>C (p.Arg284Pro) (Fig. 2A). Arg284 is conserved among many vertebrates and some invertebrates such as *Drosophila* (Fig. S1). *In silico* analysis of p.Arg284Pro in OGT predicted pathogenicity of the mutation (Table 2). The heterozygous nature of the mutation in *BRD1*, in addition to lower pathogenicity predictions for p.Val230Leu (Table 2) made this variant less likely to be pathogenic.

For patient 2, a gene panel for known intellectual disability genes and *de novo* analysis did not reveal a potential causative mutation. Further analysis of the exome data by filtering for variants following an autosomal recessive or X-linked inheritance showed a hemizygous variant in *OGT*: ChrX(GRCh38): g.71,544,561T>G; NM_181672.2: c.463-6T>G. Segregation analysis revealed that the mutation originates from a *de novo* mutation in the grandmother of the patient, passed on via the mother, who is the carrier (Fig. 2A). The thymine at position c.463-6 is highly conserved (phyloP score of 6.93) and *in silico* splicing analysis of c.463-6T>G predicted an effect on the canonical splice site. RT-PCR in patient fibroblasts showed an additional splice variant for OGT (Fig. 2B). Sanger sequencing showed a deletion of 69 base pairs, corresponding to skipping of exon 4 due to partial loss of the canonical splice site in patient 2 (Fig. 2B). Skipping of Exon 4 could result in a truncated protein with a loss of 23 amino acids (Δ 155-177-OGT).

Both mutations in OGT were absent in >60,000 controls (ExAC database) (31).

Thus, we have identified two XLID patients that possess two novel mutations in *OGT*.

OGT XLID mutations lead to an imbalance of O-GlcNAc homeostasis

Given that OGT is a glycosyltransferase we next investigated the effects of the XLID mutations on global O-GlcNAc levels in lysates from patient-derived fibroblasts by immunoblotting. As controls, we used fibroblasts from an unrelated male neonate (control 1) and a female adult (control 2). Using the RL2 anti-O-GlcNAc antibody, we observed no substantial difference in global O-GlcNAc levels between the controls and patients (Fig. 3A and 3B). To verify the specificity of this O-GlcNAc antibody, cell lysates were treated with a bacterial O-GlcNAcase from *Clostridium perfringens* (CpOGA), leading to a loss of O-GlcNAc signal compared to untreated lysates (Fig. 3A). As an independent control experiment, we applied a recently developed method to detect O-GlcNAcylated proteins, which relies on detection using a tagged inactive bacterial O-GlcNAcase (Asp298Asn-CpOGA) (32). In this experiment, no substantial differences were observed in global O-GlcNAc levels in fibroblasts derived from patients versus healthy controls (Fig. 3C and 3D).

We next investigated the effects of the *OGT* mutations on levels of OGT and OGA mRNA and protein. Gene expression levels of *OGT* and *OGA* appeared to be unaffected in patient fibroblasts compared to those of the controls (Fig. 4A). Although OGT protein levels appeared reduced in both patients compared to the healthy controls (Fig 4B and 4C), there was considerable variability in OGT protein levels of the healthy controls (Fig. 4B and 4C). At the mRNA level two OGT variants (corresponding to WT and misspliced products) were present for patient 2 (Fig. 2B). However, at the protein level, comparative analysis with recombinantly expressed Δ 155-177-OGT (Fig. 4F) did not show evidence for presence of a truncated OGT protein, suggesting that Δ 155-177-OGT may be unstable/degraded in the context of these patient fibroblasts. There was a reduction in OGA protein levels, although again variability was observed in OGA protein levels of the healthy controls (Fig. 4D and 4E). Thus, *OGT* mutations may lead to reduced functional OGT protein levels in patient-derived fibroblasts, which may be compensated for with downregulation of

OGA protein levels, thereby maintaining global *O*-GlcNAc levels.

Recombinant mutant OGT is unstable and defective in HCF-1 processing

The absence of the truncated OGT in patient 2 and potential reductions in OGT protein levels in patient-derived fibroblasts suggest that the mutations may compromise OGT stability. To further investigate this, stability of recombinant wild type/mutant OGT TPR domain was analysed by thermal denaturation experiments. We observed reduced stability for $\Delta 155-177$ -OGT ($T_m = 51 \pm 1^\circ\text{C}$) and Arg284Pro-OGT ($T_m = 52 \pm 1^\circ\text{C}$) compared with wild type OGT TPR domain ($T_m = 59 \pm 1^\circ\text{C}$) (Fig. 5A). Given that $\Delta 155-177$ -OGT was not detected in patient-derived fibroblasts, further biochemical characterisation of this mutant was omitted. OGT has over a thousand *O*-GlcNAcylation substrates, therefore, in order to explore the effects of the Arg284Pro mutation in an environment similar to that of cell physiology, de-*O*-GlcNAcylated HEK-293 cell lysate was employed as a complex array of substrates. Arg284Pro-OGT was not able to restore protein *O*-GlcNAcylation, to the extent achieved by wild type OGT (Fig. 5B).

OGT is known to possess a second catalytic activity, promoting autocatalytic cleavage and activation of the transcriptional co-regulator HCF1, itself an XLID gene (33,34), via an intermediate glycosylation step (13,35). Thus, we decided to investigate the effects of the Arg284Pro mutation on OGT-mediated HCF1 processing. To measure proteolytic activity, we used a GST-fusion of a minimal HCF1 fragment (HCF1-rep1) possessing the first of the PRO-repeats (which are the target sites of proteolysis, Fig. 5C). Wild type OGT was able to hyperglycosylate HCF1-rep1, as evidenced by a band shift that was reversible by incubation with CpOGA (Fig. 5D). The HCF1-rep1 band shift observed in the Arg284Pro-OGT-catalysed reaction was smaller, suggesting that the mutant OGT was less effective than the wild type in glycosylating HCF1-rep1 (Fig. 5D). Furthermore, wild type OGT was able to induce auto-proteolysis, whereas the proteolytic activity of Arg284Pro-OGT was reduced (Fig. 5D). When the enzyme concentration was reduced relative to substrate levels, proteolytic activity of Arg284Pro-OGT was abrogated, whereas wild type enzyme still displayed detectable activity (Fig. 5E). Thus, recombinant Arg284Pro-OGT is

defective in HCF1 glycosylation and proteolytic processing.

DISCUSSION

Here, we report two patients with XLID attributable to hemizygous mutations in *OGT*: one missense mutation (Arg284Pro) and one splice-site mutation (c.463-6T>G). We identified potential perturbations in protein *O*-GlcNAc homeostasis in both patients and altered HCF1 maturation in patient 1.

XLID is a genetically and phenotypically heterogeneous group of disorders, estimated to account for approximately 10% of all intellectual disability phenotypes in males (36). Mutations causing XLID have been reported in over 100 genes, and new XLID genes are still being identified (37). In 2015, Niranjan et al. published a series of 65 potential XLID genes, by sequencing the X-exome of 56 XLID families (30). This was the first publication in which a genetic variant in *OGT* (p.Leu254Phe) was found associated with XLID. During the course of our work, Vaidyanathan et al. (38) reported a study on the functional characterisation of this previously published p.Leu254Phe variant of OGT (30). In patient derived lymphoblastoid cells, decreased OGT levels were accompanied by decreased OGA levels, resulting in unaltered *O*-GlcNAc levels. This is in agreement with our findings in both patient-derived fibroblast cell lines, indicating that homeostasis of *O*-GlcNAc levels through decreasing OGA could be a general principle in cases of OGT deficiency. However in contrast to our results, recombinantly expressed p.Leu254Phe OGT and wild type OGT showed equal activity towards *O*-GlcNAc substrate CK2 α and HCF-1 (38). Another study described a missense mutation in *OGT* (p.Ala319Thr) in an XLID family, although this mutant also segregated with a previously uncharacterised variant of *MED12*, another gene that is associated with XLID. Evidence for functional loss of OGT for this mutation was not provided (29).

To date, including our findings, four hemizygous mutations in *OGT* have been identified in patients with XLID (Table 1). The three missense mutations (p.Arg284Pro, p.Leu254Phe and p.Ala319Thr) and one splice-site mutation (c.463-6T>G) all affect the N-terminal TPR domain (Fig. 2C and S1). The TPR motif is characterised by a repeat of 34 amino acids that fold into two antiparallel helices. The TPR domain consists of 13.5 repeats and the

antiparallel helices align to form an elongated superhelix, where the first helix of each TPR repeat (helix A) faces towards the inner surface of the elongated superhelix and their antiparallel pairs (helix B) form the outer surface (11). The missense mutations p.Arg284Pro, p.Leu254Phe and p.Ala319Thr are located in helix B of the OGT TPRs7, 8 and 9, respectively (Fig. 2D and S1). In addition, Ala319 is one of the conserved hydrophobic amino acid residues of the canonical TPR repeat (39) (Fig. S1). Each of these missense mutations could disrupt the α -helical secondary structure of the TPR domain, thereby affecting the overall stability of the elongated superhelix (Fig. 2D). The Arg284 is located in the middle of TPR helix 7B, and mutation of this residue to a Pro likely disrupts this secondary structure element, destabilising this region.

The splice-site mutation c.463-6T>G is predicted to result in an OGT protein missing 23 amino acids (p. Δ 155-177) (Fig. 2B), although we could not confirm the presence of a truncated OGT in patient fibroblasts (Fig. 4F). We propose that this mutation might exert its effect by producing an unstable splice variant and reducing the amount of functional OGT within the cell (Fig. 4B and 5A). Global *O*-GlcNAc levels in patient-derived fibroblasts were not substantially reduced compared to healthy controls (Fig 3). Protein levels of OGT and OGA appeared to be reduced in both patients, however both healthy controls displayed variation in their OGT and OGA levels, complicating the interpretation of these findings. We hypothesize that the decrease in OGT protein levels in these cells might be counteracted by the concomitant reduction of OGA protein levels (Fig. 4D and 4E), thereby sustaining basal *O*-GlcNAc homeostasis. This hypothesis is supported by the finding that chemical inhibition of OGA in different human cell lines leads to a decreased expression of OGT and an increased expression of OGA (18), which indicates an as yet unidentified mechanism of regulation to maintain global *O*-GlcNAc homeostasis. We propose a similar mechanism in our patient-derived fibroblasts.

It is as yet not fully understood how OGT recognises serines/threonines on specific proteins for *O*-GlcNAcylation, although there is evidence to suggest that the TPRs play a key role for at least a subset of substrates (40). To assess the *in vitro* activity of OGT with mutations affecting the TPR domain and the impact on

substrate *O*-GlcNAcylation, we produced recombinant Arg284Pro-OGT. Given that Δ 155-177-OGT was not detected in patient-derived fibroblasts, further biochemical characterisation of this mutant was not undertaken. Activity assays against de-*O*-GlcNAcylated HEK-293 lysate demonstrated that the p.Arg284Pro mutation led to a global reduction in protein *O*-GlcNAcylation, as opposed to reducing recognition and *O*-GlcNAcylation of specific substrates. In a physiological context, this non-specific reduction in OGT activity may be rescued by down-regulation of OGA levels, which was observed to some extent in the fibroblasts from both patients. However, the p.Arg284Pro mutation is located on the surface of the TPRs (11), a region that has been shown to play a role in the recognition of specific substrates (40). It is therefore possible that this mutation could affect modification of specific substrates, in addition to causing the observed global reduction in substrate *O*-GlcNAcylation, and this possibility is neither excluded nor confirmed by our current data. *O*-GlcNAcylation activity of Arg284Pro-OGT against HCF1-rep1 was reduced, as judged by the poly-*O*-GlcNAcylation-induced shift in HCF1-rep1 molecular weight versus wild type OGT (Fig. 5D).

In addition to being abundantly *O*-GlcNAcylated (15), HCF1 is also proteolytically processed by OGT (12,35). The Arg284Pro mutation appears to alter HCF1-rep1 proteolysis *in vitro* (Fig. 5D and 5E). The TPR domain is critical for proteolytic maturation of HCF1 (13) and this could explain why Arg284Pro-OGT shows decreased proteolytic activity towards HCF1 *in vitro*. Interestingly, *HCFC1*, the gene that codes for HCF1, is located on the X-chromosome and it is reported as an XLID gene (41). This hints at possible overlap in downstream disease mechanisms causing intellectual disability in patients bearing *OGT* or *HCFC1* mutations.

Precisely how alterations in protein *O*-GlcNAcylation and HCF1 cleavage lead to intellectual disability is not yet clear. OGT is expressed in a broad range of tissues, with a remarkably high expression in brain (9,10). *O*-GlcNAc modified proteins were detected in nerve terminals and abundant OGT activity was detected in nerve synaptosomes (42), indicating that *O*-GlcNAc could play a role in neuronal function and neurodegenerative disease. It has been suggested that regulation of the proteasome

complex by *O*-GlcNAcylation in the brain could contribute to apoptosis of hippocampal cells, and thus neurodegeneration (43). In addition, aberrant *O*-GlcNAcylation levels have been linked to neurodegenerative diseases like Alzheimer's disease (28). Future work analysing the effect of XLID mutations on OGT function in a more phenotype-relevant model, such as a neuronal cell line or an animal model where the effect of the mutations on different tissues, including the brain, can be investigated, would be important. The present study utilised fibroblasts from two unrelated individuals as controls, and we noted substantial variability in OGA and OGT protein levels in these cells, complicating the interpretation of our data. In order to minimise the effect of variability introduced by the differing genetic background between individual patients and controls, it would be of use to introduce these mutations into cell lines with an identical genetic background. .

Our study provides the first detailed clinical characterisation of patients with XLID attributable to mutations in OGT, and furthermore, proposes a potential molecular explanation for how these mutations may impact on OGT dual function of *O*-GlcNAcylation and HCF1 proteolysis.

EXPERIMENTAL PROCEDURES

Patient consent

Exome sequencing and use of patient facial images was done with written informed consent.

Whole exome sequencing

For patient 1, whole exome sequencing was performed in a trio diagnostic approach as described before (44). Exome capture was performed with the SureSelect Human All Exon v4 enrichment kit (Agilent, CA, USA). Whole exome sequencing was performed on the Illumina HiSeq platform (CA, USA). Data were analysed with BWA (read alignment) and GATK (variant calling) software packages. Variants were annotated using an in-house developed pipeline. Prioritization of variants was done by an in-house designed 'variant interface' and manual curation.

Exomes of patient 2 and parents were enriched using the SureSelect XT Human All Exon V5 kit (Agilent) and sequenced in rapid run mode on the HiSeq2500 sequencing system (Illumina) at a mean target depth of 100X. The target is defined as all coding exons of UCSC and Ensembl +/-

20bp intron flanks. At this depth >95% of the target is covered at least 15X. Reads were aligned to hg19 using BWA (BWA-MEM v0.7.5a) and variants were called using the GATK haplotype caller (v2.7-2). Detected variants were annotated, filtered and prioritized using the Bench NGS Lab platform (Cartagenia, Agilent). *OGT* gene sequences of grandmother and great-grandmother were analysed to study the origin of the mutation. All potentially causative variants were confirmed by Sanger sequencing.

Cell Culture

Skin fibroblasts derived from patients and healthy donors were cultured at 37 °C under 5.0% CO₂ in M199 medium (PAN biotech, Aidenbach, Germany) or Dulbecco's Modified Eagle Medium (Thermo Fisher Scientific, MA, USA) containing 2 mM L-glutamine (Sigma, MO, USA). Media were supplemented with 10% Foetal Calf Serum (Labtech, Uckfield, UK) and 1% Penicillin-Streptomycin (Thermo Fisher Scientific).

RNA extraction, cDNA synthesis and (q)RT-PCR

Total cell RNA was extracted from skin fibroblasts using TRIzol reagent (Thermo Fisher Scientific). cDNA was synthesized with RevertAid First Strand cDNA Synthesis Kit (Thermo Fisher Scientific) using random hexamer primers. For quantification of OGT and OGA expression levels, cDNA from skin fibroblasts was mixed with GoTaq® qPCR Master Mix (Promega, WI, USA) and both forward and reverse primers. Tubulin expression was used as an internal control. All qPCR experiments were conducted at Biorad CFX96 Real-Time System following the GoTaq® qPCR Master Mix manual. Specificity of the reactions was verified with melt curve analysis. Primers used are listed in table S1. For analysis of OGT mRNA splicing in skin fibroblasts of patient 2, cDNA and primers were mixed with AmpliTaq Gold® 360 Master Mix (Thermo Fisher Scientific). RT-PCR was conducted according to standard conditions and PCR products were purified using QIAquick Gel Extraction Kit (Qiagen, Hilden, Germany). Purified PCR products were used for sequencing analysis.

Biochemical characterization of patient-derived fibroblasts

Patient-derived fibroblasts were grown on 15 cm plates and were washed twice with ice cold PBS

buffer (Thermo Fisher Scientific) prior to lysis. Cells were lysed by addition of lysis buffer (50 mM Tris-HCl, pH 7.4, 1 mM EGTA, 1 mM EDTA, 1% Triton-X100, 1 mM Na₃VO₄, 50 mM NaF, 5 mM pyrophosphate, 0.27 M sucrose) supplemented with 1 μ M GlcNAcstatin-G, 1 μ M β -mercaptoethanol and protease inhibitor cocktail (1 mM benzamidine, 0.2 mM PMSF, 5 mM leupeptin). The lysate was transferred into an Eppendorf and clarified by centrifugation at 4 °C (1200 g for 15 min). Lysate proteins were resolved by SDS-PAGE (4-12% acrylamide [Thermo Fisher Scientific]) and transferred onto nitrocellulose membranes (GE Healthcare, IL, USA). Analysis of *O*-GlcNAcylated fibroblast proteins by the far Western method was performed as described previously (32). Briefly, soluble cell lysates were prepared, resolved by SDS-PAGE (3-8% Tris-acetate [Thermo Fisher Scientific] and transferred onto nitrocellulose membranes (GE Healthcare) as described above, but with lysis buffer lacking GlcNAcstatin-G.

Protein expression and purification

Full length wild type OGT and mutants (Arg284Pro and Δ 155-177) were expressed in *E. coli* as N-terminal His fusion proteins as described previously (45). The wild type OGT TPR domain (residues 16-410) and mutants (TPR-Arg284Pro and TPR- Δ 155-177) were expressed and purified as described previously (11). HCF1-rep1 (residues 867-1071) was expressed in *E. coli* as a non-cleavable N-terminal GST and C-terminal His fusion protein. Transformed BL21 (DE3) cells were grown, induced for expression, lysed and clarified as described previously (45). Clarified lysate was incubated with 1 ml/L of culture of Glutathione Sepharose 4B resin (GE Healthcare) for 2 h at 4 °C. The resin was thoroughly washed with base buffer (0.1 M Tris-HCl, pH 7.5, 150 mM NaCl, 0.5 mM TCEP) and eluted using base buffer supplemented with 0.5 M glutathione. Eluted protein was dialyzed overnight at 4 °C in buffer A (0.1 M Tris-HCl, pH 7.5, 25 mM NaCl). Dialyzed protein was passed through 5 ml HiTrap Q Sepharose FF anion exchange resin (GE Healthcare), collecting the flow-through, which was then concentrated and passed through a 300 ml SuperdexTM 200 column (GE Healthcare) pre-equilibrated with base buffer. The peak fractions were concentrated to 10 mg/ml, mixed 1:1 with 50% glycerol, snap-frozen and stored at -80 °C until use.

Molecular cloning

The fragment of HCF1-rep1 (residues 867-1071) was obtained from MVP Human total Brain RNA from Agilent using the Takara PrimeScript High Fidelity RT-PCR Kit. The reverse primer coded for the C-terminal addition of a 6His tag. The PCR product was cloned as a *Bam*HI-*Not*I fragment into a mutated version of pGEX6P1 which lacks the PreScission protease site. The full length codon optimised OGT was obtained from GenScript and sub cloned as a *Bam*HI-*Not*I fragment into pHEX6P1 (modified version of pGEX6P1 which contains a 6His tag instead of GST). The Arg284Pro and the Δ 155-177 mutations were introduced using a method similar to the QuikChange site-directed mutagenesis kit (Agilent) but using KOD polymerase and *Dpn*I from Fermentas. All inserts were confirmed by DNA sequencing.

Thermal denaturing assay

Thermal denaturing experiments were performed in triplicate, using the OGT TPR domain constructs. 50 μ l solutions contained 5 μ M protein and 1.1x SYPRO[®] Orange dye (Sigma) in base buffer of 25 mM HEPES-NaOH pH 7.5, 150 mM NaCl and 0.5 mM TCEP. A BioRad (CFX ConnectTM) Real-Time System was used to measure fluorescence (λ_{ex} = 530 nm, λ_{em} = 560 nm) while temperature was increased from 25 to 95 °C at 1 degree per minute increments. The data was transformed, normalised and fitted to a Boltzmann sigmoidal curve using GraphPad Prism 5.0.

In vitro O-GlcNAcylation assay

O-GlcNAcylation assays were performed in triplicate on de-*O*-GlcNAcylated HEK-293 lysate proteins. HEK-293 cell lysates were prepared as described for patient-derived fibroblasts, but with the lysis buffer lacking GlcNAcstatin-G. HEK-293 lysate was treated with 120 μ g *Cp*OGA per mg of lysate protein and incubated for 90 minutes at 37 °C. *Cp*OGA was neutralised by addition of 250 μ M GlcNAcstatin-G. Reactions were supplemented with wild type OGT or Arg284Pro-OGT (0.2 μ M) in presence of 2 mM UDP-GlcNAc and incubated for an additional 2 h at 37 °C. Proteins were resolved by SDS-PAGE (3-8% acrylamide [Thermo Fisher Scientific]) and transferred onto nitrocellulose membrane (GE Healthcare).

In vitro proteolytic assay

Proteolytic assays were performed using HCF1-rep1 (residues 867-1071) with GST and His tags at the N-terminus and C-terminus, respectively. For qualitative measurement of proteolytic activity, HCF1-rep1 (2.5 μ M), pre-incubated or not with CpOGA (5 μ M), was combined with wild type OGT or Arg284Pro-OGT (1 μ M) in the presence of 1 mM UDP-GlcNAc. Reaction mixtures were incubated at 37 °C for 8 h with gentle agitation, followed by optional addition of CpOGA. Mixtures were incubated at 37 °C for an additional 1 h, before stopping the reaction by addition of LDS loading buffer (4X) (Thermo Fisher Scientific). Proteins were resolved by SDS-PAGE (4-12% acrylamide [Life Technologies]) and transferred onto nitrocellulose membranes (GE Healthcare). Initial velocity for OGT-catalysed proteolysis of HCF1-rep1 was measured in triplicate. HCF1-rep1 (1.5 μ M) was combined with wild type OGT or Arg284Pro-OGT (0.15 μ M) in the presence of 150 μ M UDP-GlcNAc. Reaction mixtures were incubated at 37 °C with gentle agitation, while aliquots were taken out at designated time-points (0, 0.5, 1, 2, 4, 8, 16 and 32 h) and stopped by mixing with LDS loading buffer (4X) (Thermo Fisher Scientific). The initial volume of the reaction was 90 μ l and 2.5 μ l aliquots were loaded in each lane. Proteins were resolved by SDS-PAGE (10% acrylamide), visualized by Coomassie staining. Amount of product formed was quantified using a LI-COR

Odyssey scanner and associated quantification software. Data was background corrected and plotted using GraphPad Prism 5.0.

Immunoblots

Membranes were probed with following primary antibodies: O-GlcNAc (RL2 [Abcam, Cambridge, UK]), actin (Sigma), OGT (H300 [Santa Cruz, TX, USA]), OGA (14711-1-AP [Proteintech, IL, USA]), tubulin (Cell Signalling), HSP-90 (Cell Signalling, MA, USA) and GST-S902 (DSTT). In case of the far Western method, membranes were probed with 10 μ g/ml Halo-tagged CpOGA. and incubated with halo primary antibody (Promega). Subsequently all membranes were incubated with IR680- or IR800-labelled secondary antibodies (LI-COR) and analysed using a LI-COR Odyssey scanner and associated quantification software. All primary and secondary antibodies were used in 1:5,000 and 1:10,000 dilutions respectively.

Data analysis

Scatter plots indicate ratios of any given normalised signal as averaged from three biological replicates, with the error bars representing standard deviation. Variation in data was calculated by Mann-Whitney U test using Graphpad Prism 5.0. Power calculations were performed using G*Power 3.1.

ACKNOWLEDGEMENTS

We would like to thank both patients and their families for participation in this study. This work was financially supported by the Dutch Organization for Scientific Research ZONMW [VIDI grant 91713359 to D.J.L.] and by a Wellcome Trust Investigator Award (110061) to D.M.F.v.A. MG was supported by a University of Dundee Translational Medical Research Fund Ph.D. fellowship. In addition, we are grateful for protein production team at Division of Signal Transduction Therapy (DSTT), the University of Dundee for production of the anti-GST antibody.

CONFLICT OF INTEREST

The authors declare that they have no conflicts of interest with the contents of this article.

AUTHOR CONTRIBUTIONS

AW and MG designed, performed and analyzed the experiments and wrote the paper. MK, JG, BL and JF provided clinical data of the patients. RP, ME and KvG performed exome sequencing and provided genetic details of the patients. AF performed molecular cloning to obtain recombinantly expressed OGT forms. DL and DvA conceived and coordinated the study and revised the paper. All authors contributed to writing of the paper, reviewing the results and approved the final version of the manuscript.

REFERENCES

1. Jackson, S. P., and Tjian, R. (1988) O-glycosylation of eukaryotic transcription factors: implications for mechanisms of transcriptional regulation. *Cell* **55**, 125-133
2. Hanover, J. A., Cohen, C. K., Willingham, M. C., and Park, M. K. (1987) O-linked N-acetylglucosamine is attached to proteins of the nuclear pore. Evidence for cytoplasmic and nucleoplasmic glycoproteins. *The Journal of biological chemistry* **262**, 9887-9894
3. Yang, W. H., Kim, J. E., Nam, H. W., Ju, J. W., Kim, H. S., Kim, Y. S., and Cho, J. W. (2006) Modification of p53 with O-linked N-acetylglucosamine regulates p53 activity and stability. *Nature cell biology* **8**, 1074-1083
4. Sayat, R., Leber, B., Grubac, V., Wiltshire, L., and Persad, S. (2008) O-GlcNAc-glycosylation of beta-catenin regulates its nuclear localization and transcriptional activity. *Experimental cell research* **314**, 2774-2787
5. Torres, C. R., and Hart, G. W. (1984) Topography and polypeptide distribution of terminal N-acetylglucosamine residues on the surfaces of intact lymphocytes. Evidence for O-linked GlcNAc. *The Journal of biological chemistry* **259**, 3308-3317
6. Haltiwanger, R. S., Blomberg, M. A., and Hart, G. W. (1992) Glycosylation of nuclear and cytoplasmic proteins. Purification and characterization of a uridine diphospho-N-acetylglucosamine:polypeptide beta-N-acetylglucosaminyltransferase. *The Journal of biological chemistry* **267**, 9005-9013
7. Ruan, H. B., Singh, J. P., Li, M. D., Wu, J., and Yang, X. (2013) Cracking the O-GlcNAc code in metabolism. *Trends in endocrinology and metabolism: TEM* **24**, 301-309
8. Hart, G. W., Housley, M. P., and Slawson, C. (2007) Cycling of O-linked beta-N-acetylglucosamine on nucleocytoplasmic proteins. *Nature* **446**, 1017-1022
9. Kreppel, L. K., Blomberg, M. A., and Hart, G. W. (1997) Dynamic glycosylation of nuclear and cytosolic proteins. Cloning and characterization of a unique O-GlcNAc transferase with multiple tetratricopeptide repeats. *The Journal of biological chemistry* **272**, 9308-9315
10. Lubas, W. A., Frank, D. W., Krause, M., and Hanover, J. A. (1997) O-Linked GlcNAc transferase is a conserved nucleocytoplasmic protein containing tetratricopeptide repeats. *The Journal of biological chemistry* **272**, 9316-9324
11. Jinek, M., Rehwinkel, J., Lazarus, B. D., Izaurralde, E., Hanover, J. A., and Conti, E. (2004) The superhelical TPR-repeat domain of O-linked GlcNAc transferase exhibits structural similarities to importin alpha. *Nature structural & molecular biology* **11**, 1001-1007

12. Capotosti, F., Guernier, S., Lammers, F., Waridel, P., Cai, Y., Jin, J., Conaway, J. W., Conaway, R. C., and Herr, W. (2011) O-GlcNAc transferase catalyzes site-specific proteolysis of HCF-1. *Cell* **144**, 376-388
13. Lazarus, M. B., Jiang, J., Kapuria, V., Bhuiyan, T., Janetzko, J., Zandberg, W. F., Vocadlo, D. J., Herr, W., and Walker, S. (2013) HCF-1 is cleaved in the active site of O-GlcNAc transferase. *Science* **342**, 1235-1239
14. Zargar, Z., and Tyagi, S. (2012) Role of host cell factor-1 in cell cycle regulation. *Transcription* **3**, 187-192
15. Myers, S. A., Daou, S., Affar el, B., and Burlingame, A. (2013) Electron transfer dissociation (ETD): the mass spectrometric breakthrough essential for O-GlcNAc protein site assignments—a study of the O-GlcNAcylated protein host cell factor C1. *Proteomics* **13**, 982-991
16. Kapuria, V., Rohrig, U. F., Bhuiyan, T., Borodkin, V. S., van Aalten, D. M., Zoete, V., and Herr, W. (2016) Proteolysis of HCF-1 by Ser/Thr glycosylation-incompetent O-GlcNAc transferase:UDP-GlcNAc complexes. *Genes & development* **30**, 960-972
17. Wells, L., Gao, Y., Mahoney, J. A., Vosseller, K., Chen, C., Rosen, A., and Hart, G. W. (2002) Dynamic O-glycosylation of nuclear and cytosolic proteins: further characterization of the nucleocytoplasmic beta-N-acetylglucosaminidase, O-GlcNAcase. *The Journal of biological chemistry* **277**, 1755-1761
18. Zhang, Z., Tan, E. P., VandenHull, N. J., Peterson, K. R., and Slawson, C. (2014) O-GlcNAcase Expression is Sensitive to Changes in O-GlcNAc Homeostasis. *Frontiers in endocrinology* **5**, 206
19. Hanover, J. A., Forsythe, M. E., Hennessey, P. T., Brodigan, T. M., Love, D. C., Ashwell, G., and Krause, M. (2005) A Caenorhabditis elegans model of insulin resistance: altered macronutrient storage and dauer formation in an OGT-1 knockout. *Proceedings of the National Academy of Sciences of the United States of America* **102**, 11266-11271
20. Ingham, P. W. (1984) A gene that regulates the bithorax complex differentially in larval and adult cells of Drosophila. *Cell* **37**, 815-823
21. Mariappa, D., Zheng, X., Schimpl, M., Raimi, O., Ferenbach, A. T., Muller, H. A., and van Aalten, D. M. (2015) Dual functionality of O-GlcNAc transferase is required for Drosophila development. *Open biology* **5**, 150234
22. Webster, D. M., Teo, C. F., Sun, Y., Wloga, D., Gay, S., Klonowski, K. D., Wells, L., and Dougan, S. T. (2009) O-GlcNAc modifications regulate cell survival and epiboly during zebrafish development. *BMC developmental biology* **9**, 28
23. Wang, A. C., Jensen, E. H., Rexach, J. E., Vinters, H. V., and Hsieh-Wilson, L. C. (2016) Loss of O-GlcNAc glycosylation in forebrain excitatory neurons induces neurodegeneration. *Proceedings of the National Academy of Sciences of the United States of America*
24. Rexach, J. E., Clark, P. M., Mason, D. E., Neve, R. L., Peters, E. C., and Hsieh-Wilson, L. C. (2012) Dynamic O-GlcNAc modification regulates CREB-mediated gene expression and memory formation. *Nature chemical biology* **8**, 253-261
25. Su, C., and Schwarz, T. L. (2017) O-GlcNAc Transferase is Essential for Sensory Neuron Survival and Maintenance. *The Journal of neuroscience : the official journal of the Society for Neuroscience*
26. Taylor, E. W., Wang, K., Nelson, A. R., Bredemann, T. M., Fraser, K. B., Clinton, S. M., Puckett, R., Marchase, R. B., Chatham, J. C., and McMahon, L. L. (2014) O-GlcNAcylation of AMPA receptor GluA2 is associated with a novel form of long-term depression at hippocampal synapses. *The Journal of neuroscience : the official journal of the Society for Neuroscience* **34**, 10-21
27. Lagerlof, O., Hart, G. W., and Huganir, R. L. (2017) O-GlcNAc transferase regulates excitatory synapse maturity. *Proceedings of the National Academy of Sciences of the United States of America* **114**, 1684-1689
28. Zheng, B. W., Yang, L., Dai, X. L., Jiang, Z. F., and Huang, H. C. (2016) Roles of O-GlcNAcylation on amyloid-beta precursor protein processing, tau phosphorylation, and hippocampal synapses dysfunction in Alzheimer's disease. *Neurological research* **38**, 177-186

29. Bouazzi, H., Lesca, G., Trujillo, C., Alwasiyah, M. K., and Munnich, A. (2015) Nonsyndromic X-linked intellectual deficiency in three brothers with a novel MED12 missense mutation [c.5922G>T (p.Glu1974His)]. *Clinical case reports* **3**, 604-609
30. Niranjana, T. S., Skinner, C., May, M., Turner, T., Rose, R., Stevenson, R., Schwartz, C. E., and Wang, T. (2015) Affected kindred analysis of human X chromosome exomes to identify novel X-linked intellectual disability genes. *PloS one* **10**, e0116454
31. Lek, M., Karczewski, K. J., Minikel, E. V., Samocha, K. E., Banks, E., Fennell, T., O'Donnell-Luria, A. H., Ware, J. S., Hill, A. J., Cummings, B. B., Tukiainen, T., Birnbaum, D. P., Kosmicki, J. A., Duncan, L. E., Estrada, K., Zhao, F., Zou, J., Pierce-Hoffman, E., Berghout, J., Cooper, D. N., Deflaux, N., DePristo, M., Do, R., Flannick, J., Fromer, M., Gauthier, L., Goldstein, J., Gupta, N., Howrigan, D., Kiezun, A., Kurki, M. I., Moonshine, A. L., Natarajan, P., Orozco, L., Peloso, G. M., Poplin, R., Rivas, M. A., Ruano-Rubio, V., Rose, S. A., Ruderfer, D. M., Shakir, K., Stenson, P. D., Stevens, C., Thomas, B. P., Tiao, G., Tusie-Luna, M. T., Weisburd, B., Won, H. H., Yu, D., Altshuler, D. M., Ardissino, D., Boehnke, M., Danesh, J., Donnelly, S., Elosua, R., Florez, J. C., Gabriel, S. B., Getz, G., Glatt, S. J., Hultman, C. M., Kathiresan, S., Laakso, M., McCarroll, S., McCarthy, M. I., McGovern, D., McPherson, R., Neale, B. M., Palotie, A., Purcell, S. M., Saleheen, D., Scharf, J. M., Sklar, P., Sullivan, P. F., Tuomilehto, J., Tsuang, M. T., Watkins, H. C., Wilson, J. G., Daly, M. J., MacArthur, D. G., and Exome Aggregation, C. (2016) Analysis of protein-coding genetic variation in 60,706 humans. *Nature* **536**, 285-291
32. Mariappa, D., Selvan, N., Borodkin, V. S., Alonso, J., Ferenbach, A. T., Shepherd, C., Navratilova, I. H., and van Aalten, D. M. (2015) A mutant O-GlcNAcase as a probe to reveal global dynamics of protein O-GlcNAcylation during Drosophila embryonic development. *The Biochemical journal* **470**, 255-262
33. Huang, L., Jolly, L. A., Willis-Owen, S., Gardner, A., Kumar, R., Douglas, E., Shoubridge, C., Wieczorek, D., Tzschach, A., Cohen, M., Hackett, A., Field, M., Froyen, G., Hu, H., Haas, S. A., Ropers, H. H., Kalscheuer, V. M., Corbett, M. A., and Gecz, J. (2012) A noncoding, regulatory mutation implicates HCFC1 in nonsyndromic intellectual disability. *American journal of human genetics* **91**, 694-702
34. Yu, H. C., Sloan, J. L., Scharer, G., Brebner, A., Quintana, A. M., Achilly, N. P., Manoli, I., Coughlin, C. R., 2nd, Geiger, E. A., Schneck, U., Watkins, D., Suormala, T., Van Hove, J. L., Fowler, B., Baumgartner, M. R., Rosenblatt, D. S., Venditti, C. P., and Shaikh, T. H. (2013) An X-linked cobalamin disorder caused by mutations in transcriptional coregulator HCFC1. *American journal of human genetics* **93**, 506-514
35. Janetzko, J., Trauger, S. A., Lazarus, M. B., and Walker, S. (2016) How the glycosyltransferase OGT catalyzes amide bond cleavage. *Nature chemical biology*
36. Ropers, H. H., and Hamel, B. C. (2005) X-linked mental retardation. *Nature reviews. Genetics* **6**, 46-57
37. Hu, H., Haas, S. A., Chelly, J., Van Esch, H., Raynaud, M., de Brouwer, A. P., Weinert, S., Froyen, G., Frints, S. G., Laumonnier, F., Zemojtel, T., Love, M. I., Richard, H., Emde, A. K., Bienek, M., Jensen, C., Hambrock, M., Fischer, U., Langnick, C., Feldkamp, M., Wissink-Lindhout, W., Lebrun, N., Castelnau, L., Rucci, J., Montjean, R., Dorseuil, O., Billuart, P., Stuhlmann, T., Shaw, M., Corbett, M. A., Gardner, A., Willis-Owen, S., Tan, C., Friend, K. L., Belet, S., van Roozendaal, K. E., Jimenez-Pocquet, M., Moizard, M. P., Ronce, N., Sun, R., O'Keeffe, S., Chenna, R., van Bommel, A., Goke, J., Hackett, A., Field, M., Christie, L., Boyle, J., Haan, E., Nelson, J., Turner, G., Baynam, G., Gillessen-Kaesbach, G., Muller, U., Steinberger, D., Budny, B., Badura-Stronka, M., Latos-Bielenska, A., Ousager, L. B., Wieacker, P., Rodriguez Criado, G., Bondeson, M. L., Anneren, G., Dufke, A., Cohen, M., Van Maldergem, L., Vincent-Delorme, C., Echenne, B., Simon-Bouy, B., Kleefstra, T., Willemsen, M., Fryns, J. P., Devriendt, K., Ullmann, R., Vingron, M., Wrogemann, K., Wienker, T. F., Tzschach, A., van Bokhoven, H., Gecz, J., Jentsch, T. J., Chen, W., Ropers, H. H., and Kalscheuer, V. M. (2016) X-exome sequencing of 405 unresolved families identifies seven novel intellectual disability genes. *Molecular psychiatry* **21**, 133-148
38. Vaidyanathan, K., Niranjana, T., Selvan, N., Teo, C. F., May, M., Patel, S., Weatherly, B., Skinner, C., Opitz, J., Carey, J., Viskochil, D., Gecz, J., Shaw, M., Peng, Y., Alexov, E.,

- Wang, T., Schwartz, C., and Wells, L. (2017) Identification and Characterization of a Missense Mutation in the O-GlcNAc Transferase Gene that Segregates with X-Linked Intellectual Disability. *The Journal of biological chemistry*
39. Sikorski, R. S., Boguski, M. S., Goebel, M., and Hieter, P. (1990) A repeating amino acid motif in CDC23 defines a family of proteins and a new relationship among genes required for mitosis and RNA synthesis. *Cell* **60**, 307-317
 40. Iyer, S. P., and Hart, G. W. (2003) Roles of the tetratricopeptide repeat domain in O-GlcNAc transferase targeting and protein substrate specificity. *The Journal of biological chemistry* **278**, 24608-24616
 41. Jolly, L. A., Nguyen, L. S., Domingo, D., Sun, Y., Barry, S., Hancarova, M., Plevova, P., Vlckova, M., Havlovicova, M., Kalscheuer, V. M., Graziano, C., Pippucci, T., Bonora, E., Sedlacek, Z., and Gecz, J. (2015) HCFC1 loss-of-function mutations disrupt neuronal and neural progenitor cells of the developing brain. *Human molecular genetics* **24**, 3335-3347
 42. Cole, R. N., and Hart, G. W. (2001) Cytosolic O-glycosylation is abundant in nerve terminals. *Journal of neurochemistry* **79**, 1080-1089
 43. Liu, K., Paterson, A. J., Zhang, F., McAndrew, J., Fukuchi, K., Wyss, J. M., Peng, L., Hu, Y., and Kudlow, J. E. (2004) Accumulation of protein O-GlcNAc modification inhibits proteasomes in the brain and coincides with neuronal apoptosis in brain areas with high O-GlcNAc metabolism. *Journal of neurochemistry* **89**, 1044-1055
 44. Neveling, K., Feenstra, I., Gilissen, C., Hoefsloot, L. H., Kamsteeg, E. J., Mensenkamp, A. R., Rodenburg, R. J., Yntema, H. G., Spruijt, L., Vermeer, S., Rinne, T., van Gassen, K. L., Bodmer, D., Lugtenberg, D., de Reuver, R., Buijsman, W., Derks, R. C., Wieskamp, N., van den Heuvel, B., Ligtenberg, M. J., Kremer, H., Koolen, D. A., van de Warrenburg, B. P., Cremers, F. P., Marcelis, C. L., Smeitink, J. A., Wortmann, S. B., van Zelst-Stams, W. A., Veltman, J. A., Brunner, H. G., Scheffer, H., and Nelen, M. R. (2013) A post-hoc comparison of the utility of sanger sequencing and exome sequencing for the diagnosis of heterogeneous diseases. *Human mutation* **34**, 1721-1726
 45. Pathak, S., Alonso, J., Schimpl, M., Rafie, K., Blair, D. E., Borodkin, V. S., Schuttelkopf, A. W., Albarbarawi, O., and van Aalten, D. M. (2015) The active site of O-GlcNAc transferase imposes constraints on substrate sequence. *Nature structural & molecular biology* **22**, 744-750

TABLES

Table 1: Comparison of clinical features of patients with hemizygote *OGT* mutations

	Patient 1	Patient 2	Niranjan et al, 2015	Bouazzi et al, 2015
Genotype				
Genomic change (ChrX, GRCh38)	71,555,312G>C	71,544,561T>G	71,555,223G>T	71,555,984G>A
cDNA (NM_181672.2)	851 G>C	463-6 T>G	762 G>T	955 G>A
Protein	Arg284Pro		Leu254Phe	Ala319Thr
Phenotype				
Neurological Features				
<i>Intellectual disability</i>	+	+	+	+
<i>Developmental delay</i>	+	+	ND	+
<i>Psychomotor retardation</i>	+	+	ND	+
<i>Behavioral problems</i>	+	-	ND	+
Brain abnormalities	+	-	ND	-
Cardiac symptoms	+	+	ND	-
Dysmorphic features	+	+	ND	+
Eye abnormalities	+	+	ND	+
Genital/reproductive abnormalities	+	+	ND	-

Table 2: Prediction of pathogenicity of *de novo* mutations detected in patient 1

	BRD1 p.Val230Leu	OGT p.Arg284Pro
Align GVGD	Class C0	Class C35
SIFT	Tolerated (score 0.06)	Deleterious (score 0.01)
MutationTaster	Disease causing (p-value: 1)	Disease causing (p-value: 1)
Polyphen-2	Possibly damaging (score: 0.544)	Probably damaging (score: 0.961)

FIGURES

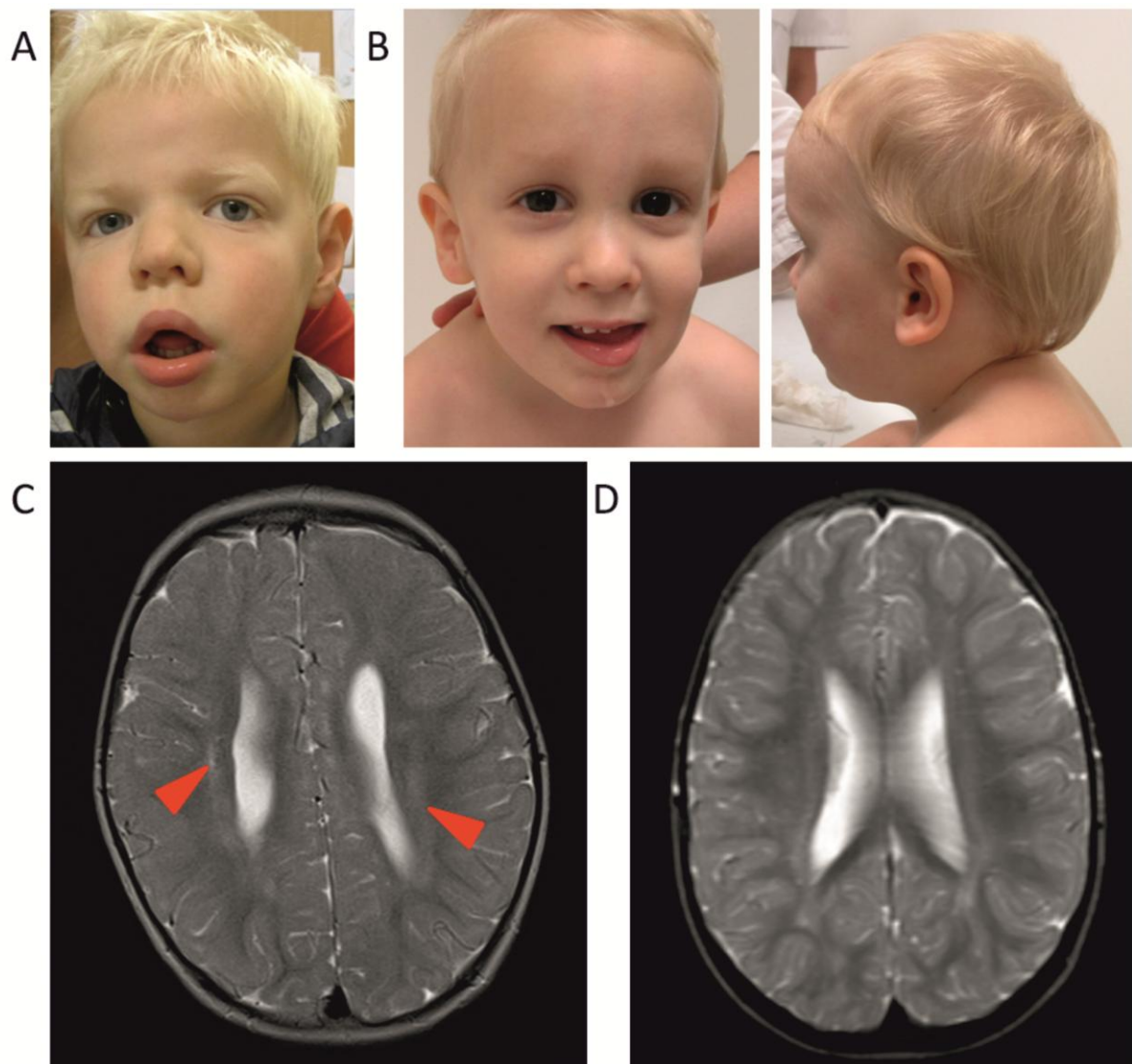


Fig. 1: Clinical images from patients with hemizygous OGT mutations

- A. Picture of patient 1, showing dysmorphic features.
- B. Pictures of patient 2, showing dysmorphic features.
- C. MRI image of patient 1, showing mild abnormalities pointing towards periventricular leukomalacia, indicated by red arrowheads.
- D. MRI image of patient 2, showing no brain abnormalities.

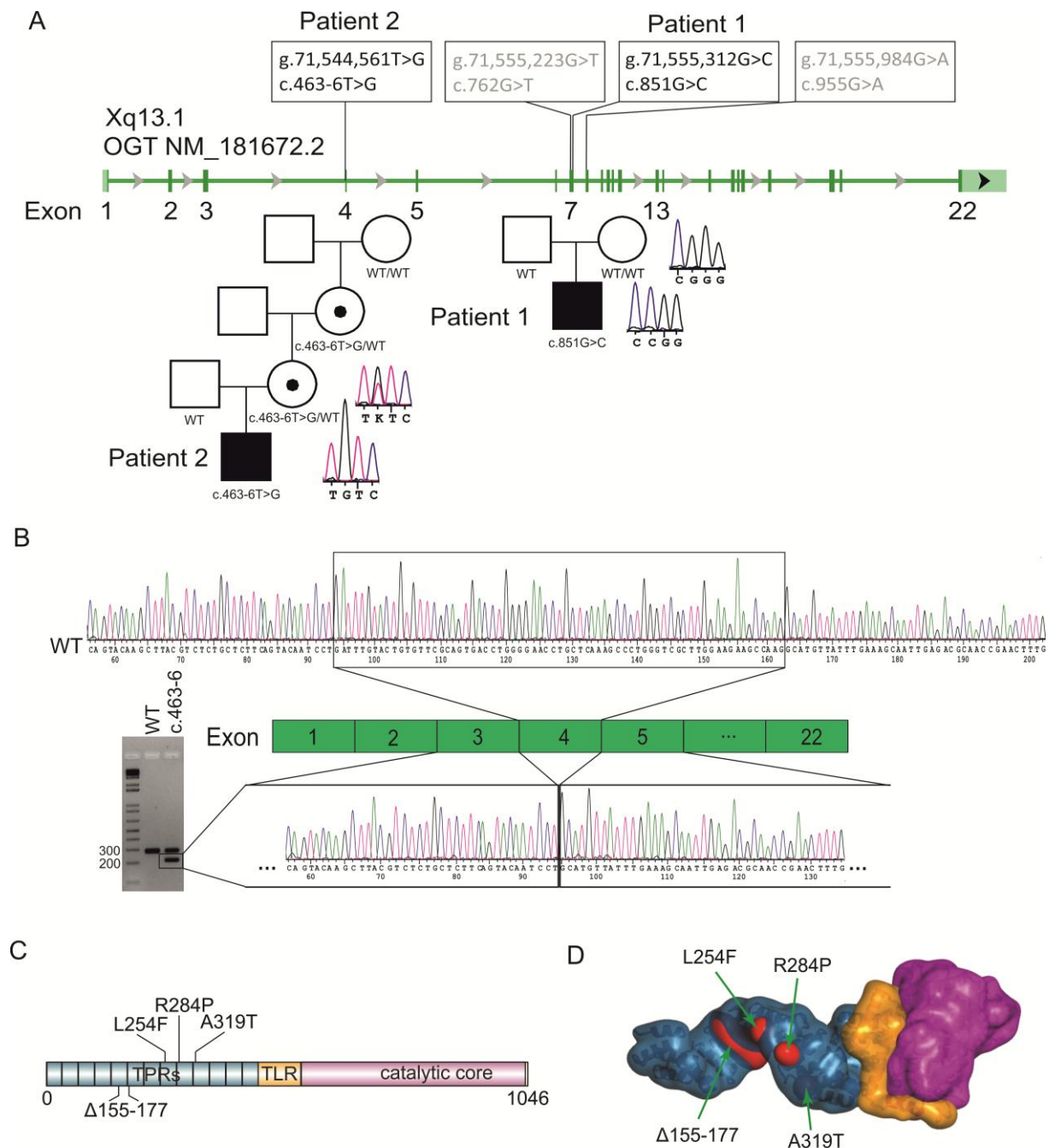


Fig. 2: Genetic analysis of hemizygous *OGT* mutations detected in patients with intellectual disability syndrome

- Location of known and newly discovered genetic variants in the *OGT* gene, and their presence in families 1 and 2.
- RT-PCR in skin-derived fibroblasts from patient 2 bearing the c.463-6T>G mutation confirmed by sequence analysis.
- Domain organization in human *O*-GlcNAc transferase. TPRs: tetratricopeptide repeats; TLR: tetratricopeptide-like repeat.
- Model for the full-length human *O*-GlcNAc transferase generated by superposition of crystallographic models for the human *O*-GlcNAc transferase catalytic domain (PDB: 5V1D) and tetratricopeptide repeat domain (PDB: 1W3B). Blue colour represents tetratricopeptide repeats, yellow colour represents tetratricopeptide-like repeat, pink colour represents catalytic core.

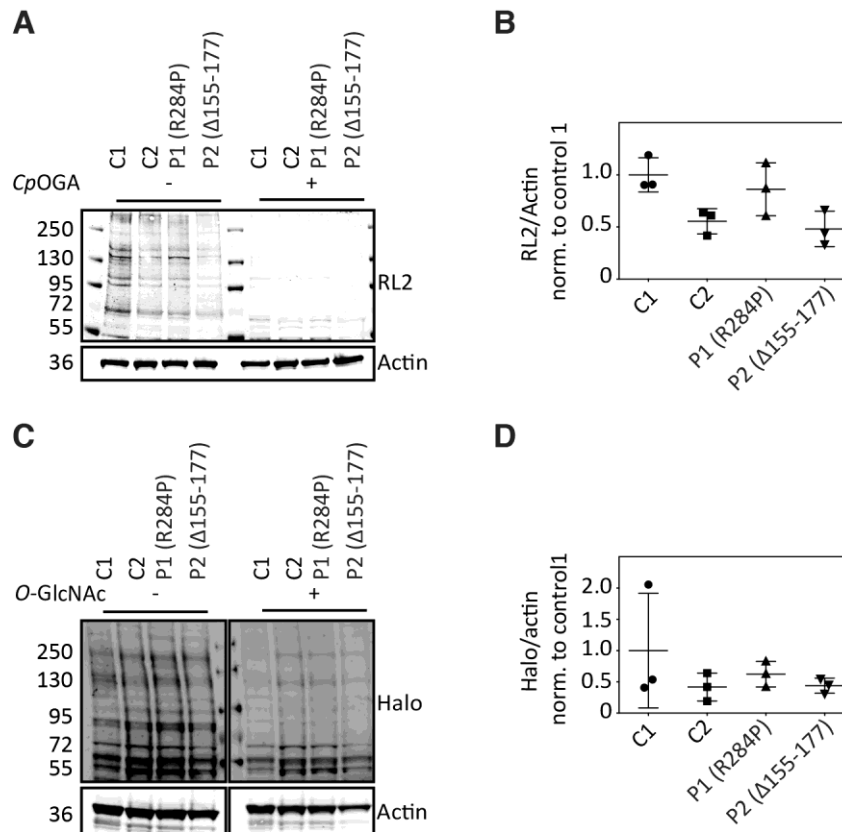


Fig. 3. Characterization of global O-GlcNAc levels in patient-derived skin fibroblasts

- Immunoblot showing global O-GlcNAc levels in patient-derived fibroblasts detected using RL2 anti O-GlcNAc antibody. C: control; P: patient.
- The scatter plot indicates fractional ratio of any given actin-normalized signal averaged from three biological replicates, with the error bars representing the standard deviation. C: control; P: patient. p-values (Mann-Whitney U test): C1-P1 = 0.4; C1-P2 = 0.1; C2-P1 = 0.4; C2-P2 = 0.9. Achieved power (1- β error probability) = 0.1
- Immunoblot showing global O-GlcNAc levels in patient-derived fibroblasts detected using the far Western method. C: control; P: patient. The far Western method relies on detection of O-GlcNAcylated protein using a point mutant of a Halo-tagged bacterial O-GlcNAcase homolog, *CpOGA*^{D298N}, as a probe (32). Halo antibody was used to detect the bands where the probe was localised.
- The scatter plot indicates fractional ratio of any given actin-normalized signal averaged from three biological replicates, with the error bars representing the standard deviation. C: control; P: patient. p-values (Mann-Whitney U test): C1-P1 = 0.9; C1-P2 = 0.7; C2-P1 = 0.7; C2-P2 = 0.9. Achieved power (1- β error probability) = 0.1

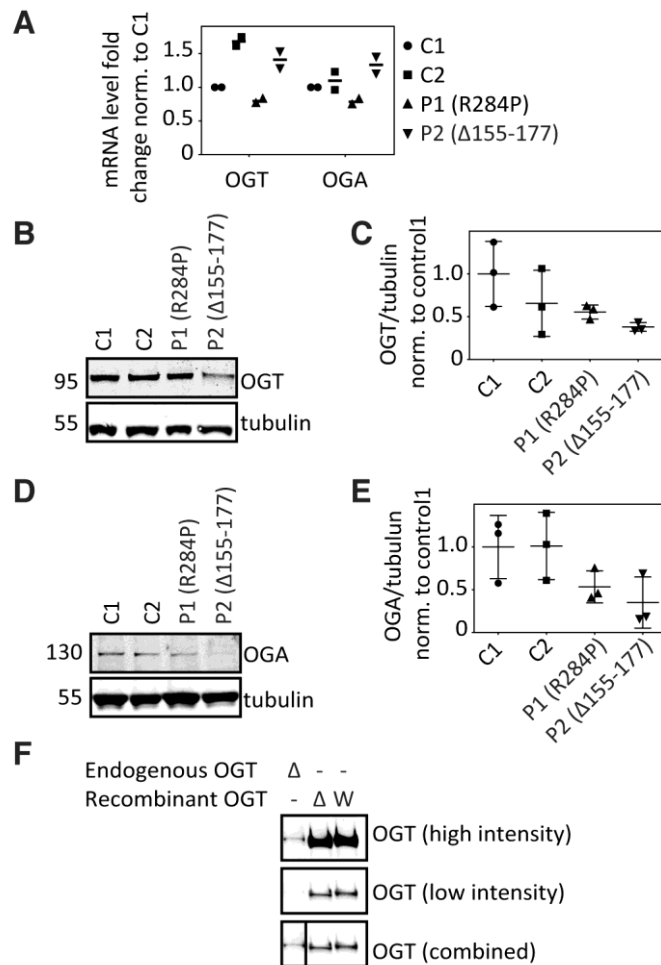


Fig. 4. Characterization of OGT and OGA levels in patient-derived skin fibroblasts

- A. Gene expression of *OGT* and *OGA* in patient fibroblasts measured by qPCR. Scatter plots represent mean data from two independent experiments. Gene expression was calculated according to $\Delta\Delta C(t)$ method. Tubulin expression was used as reference, and data were normalized against Control 1
- B. Immunoblot showing O-GlcNAc transferase (OGT) levels in patient-derived fibroblasts. C: control; P: patient.
- C. The scatter plot indicates fractional ratio of any given tubulin-normalized signal averaged from three biological replicates, with the error bars representing the standard deviation. C: control; P: patient. p-values (Mann-Whitney U test): C1-P1 = 0.9; C1-P2 = 0.1; C2-P1 = 0.9; C2-P2 = 0.7. Achieved power ($1-\beta$ error probability) = 0.1
- D. Immunoblot showing O-GlcNAcase (OGA) levels in patient-derived fibroblasts. C: control; P: patient.
- E. The scatter plot indicates fractional ratio of any given tubulin-normalized signal averaged from three biological replicates, with the error bars representing the standard deviation. C: control; P: patient. p-values (Mann-Whitney U test): C1-P1 = 0.2; C1-P2 = 0.2; C2-P1 = 0.2; C2-P2 = 0.2. Achieved power ($1-\beta$ error probability) = 0.1
- F. Immunoblot comparing OGT protein molecular weight, as present in fibroblasts of patient 2 (Δ 155-177) and of recombinantly expressed wild type OGT (W) and Δ 155-177-OGT (Δ).

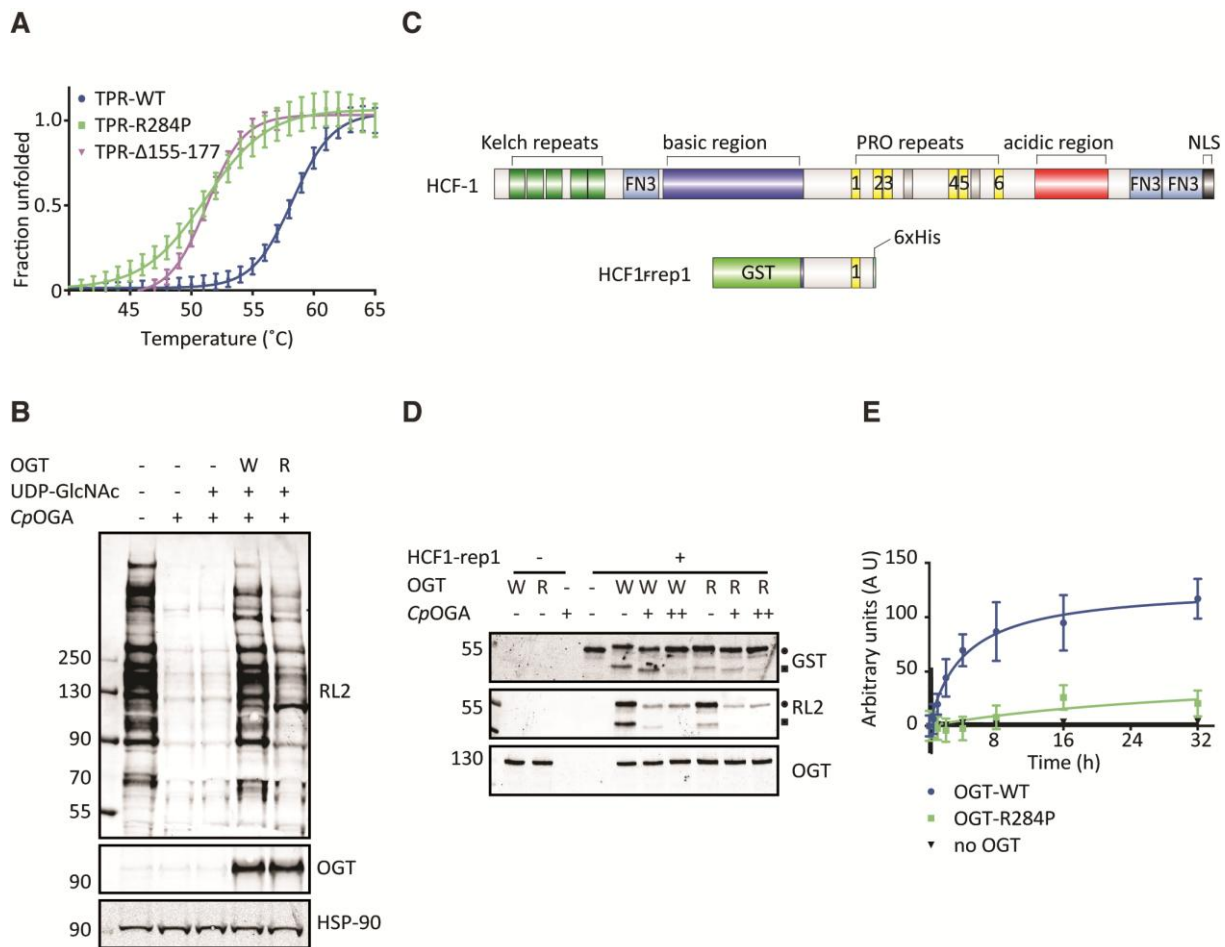


Fig. 5. *In vitro* analysis of recombinantly expressed mutant OGT forms

- Thermal denaturing curve showing fraction of unfolded wild type (TPR-WT), Arg284Pro (TPR-R284P) and $\Delta 155-177$ (TPR- $\Delta 155-177$) OGT TPR domains as a function of time. Data were fitted to Boltzmann sigmoidal curve equation. Error bars represent standard error of mean of seven replicates and the plot is representative of three biological replicates.
- Immunoblot showing the relative O-GlcNAcylation activities of wild type OGT (W) and Arg284Pro-OGT (R) against de-O-GlcNAcylated HEK-293 lysate.
- Domain organization of human host cell factor 1 (HCF1) compared to its truncated form fused to N-terminal GST-tag and C-terminal His-tag (HCF1-rep1), which was used as a substrate for OGT proteolytic activity.
- Immunoblot showing the relative proteolytic activities of wild type OGT (W) and Arg284Pro-OGT (R) against HCF1-rep1. The samples were treated with an O-GlcNAcase homologue from *Clostridium perfringens* (CpOGA) either towards the end of the reaction (+) or from the beginning (++). Closed circle: unprocessed HCF1-rep1; Closed square: HCF1-rep1 cleavage product.
- Kinetic assay of the proteolytic activity of wild type OGT and Arg284Pro-OGT against HCF1-rep1 plotted as amount of product formed as a function of time. Error bars represent standard error of mean of four replicates. Data were fitted to hyperbolic curve equation.

**Mutations in *N*-acetylglucosamine (*O*-GlcNAc) transferase in patients with
X-linked intellectual disability**

Anke P. Willems, Mehmet Gundogdu, Marlies J.E. Kempers, Jacques C. Giltay, Rolph Pfundt, Martin Elferink, Bettina F. Loza, Joris Fuijkschot, Andrew T. Ferenbach, Koen L.I. van Gassen, Daan M.F. van Aalten and Dirk J. Lefeber

J. Biol. Chem. published online June 5, 2017

Access the most updated version of this article at doi: [10.1074/jbc.M117.790097](https://doi.org/10.1074/jbc.M117.790097)

Alerts:

- [When this article is cited](#)
- [When a correction for this article is posted](#)

[Click here](#) to choose from all of JBC's e-mail alerts

Supplemental material:

<http://www.jbc.org/content/suppl/2017/06/05/M117.790097.DC1>

This article cites 0 references, 0 of which can be accessed free at

<http://www.jbc.org/content/early/2017/06/05/jbc.M117.790097.full.html#ref-list-1>